VOLUME 112, NUMBER 21
OCTOBER 10, 1990

JOURNAL
OF THE
AMERICAN
CHEMICAL
SOCIETY

^{13}C–^{31}P Cross Polarization between Isolated Spin Pairs in Organophosphorus Substances: Intramolecular Structure and Internuclear Distance Determinations in Spinning Solids

Edward W. Hagaman,* Patience C. Ho, Lloyd L. Brown, Fred M. Schell,[1] and Madge C. Woody

Contribution from the Chemistry Division, Oak Ridge National Laboratory, Oak Ridge, Tennessee 37831-6201. *Received April 2, 1990*

Abstract: Cross polarization between dilute effectively isolated ^{13}C–^{31}P spin pairs provides a unique method to examine selectively the microenvironment around the phosphorus atom in organophosphorus substances. Strong oscillations occur during cross polarization between these isolated spin pairs in MAS experiments on microcrystalline powders. The oscillation frequency is proportional to the ^{13}C–^{31}P dipolar interaction and hence allows specific internuclear distance determinations on powder samples. Maximum carbon signal intensity and experimental simplicity are achieved in double cross polarization (DCP)/MAS ^{13}C NMR experiments that impose a short $T_{1\rho}$ on the ^{31}P magnetization by ^{31}P radio frequency phase modulation. This experimental stratagem suppresses cross-polarization oscillations and yields simple exponential kinetics for the transfer process. It also relaxes the tolerance on the match condition and MAS speed for cross polarization between weakly coupled dipole pairs.

A recently reported solid-state NMR technique, ^{1}H–^{13}C–^{31}P double cross polarization (DCP)/MAS ^{13}C NMR spectroscopy, allows selective detection of the resonances of carbon centers in a ca. 0.4 nm radius spherical volume element centered on the ^{31}P atom in organophosphorus substances.[2] The resonance selection in this experiment is achieved by ^{13}C–^{31}P cross polarization between isolated spin pairs, restricting the ^{13}C NMR spectrum to the resonances of those carbons that are dipole–dipole coupled to ^{31}P nuclei. The direct difference DCP experiment has been designed such that the ^{13}C signal intensity accrues at the ^{31}P–^{13}C cross-polarization rate, $(T_{CP})^{-1}$, and decays by the rotating frame ^{13}C spin–lattice relaxation rate, ^{13}C $(T_{1\rho})^{-1}$.[3] The relative magnitude of these rates determines the sensitive volume element in which DCP signals can be observed. Resonance assignments to carbons at variable internuclear ^{31}P–^{13}C separations are made on the basis of $(T_{CP})^{-1}$'s. In this full report, salient features of ^{1}H–^{13}C–^{31}P DCP/MAS ^{13}C NMR are illustrated. Particular attention is given to the characterization of strong oscillations in the cross-polarization ^{13}C magnetization as a function of ^{13}C–^{31}P contact time. These oscillations are proportional to the ^{13}C–^{31}P dipole–dipole interaction, D_{CP}, and are used to calculate internuclear distance. ^{13}C–^{31}P cross-polarization intensity is examined as a function of the MAS-modulated Hartmann–Hahn match condition.[4]

Experimental Section

NMR. Solid-state NMR experiments were performed on a modified Nicolet Technology 4.7 T NMR spectrometer equipped with three radio frequency channels. All channels have phase $(n\pi/2)$ and amplitude (0.1-dB interval) control. In addition, the ^{31}P radio frequency channel had a continuously variable attenuator that allowed finer control (0.04 dB, oscilloscope resolution) of this radio frequency amplitude. Pulse sequence timing was controlled by the Nicolet 293B programmable

(1) Department of Chemistry, University of Tennessee, Knoxville, Knoxville, TN 37996-1600.
(2) Hagaman, E. W. *J. Am. Chem. Soc.* **1988**, *110*, 5594–5595.
(3) (a) Stejskal, E. O.; Schaefer, J.; McKay, R. A. *J. Magn. Reson.* **1984**, *57*, 471–485. (b) Schaefer, J.; Stejskal, E. O.; Garbow, J. R.; Mckay, R. A. *J. Magn. Reson.* **1984**, *59*, 150–156.
(4) Hartmann, S. R.; Hahn, E. L. *Phys. Rev.* **1962**, *128*, 2042–2053.

0002-7863/90/1512-7445$02.50/0

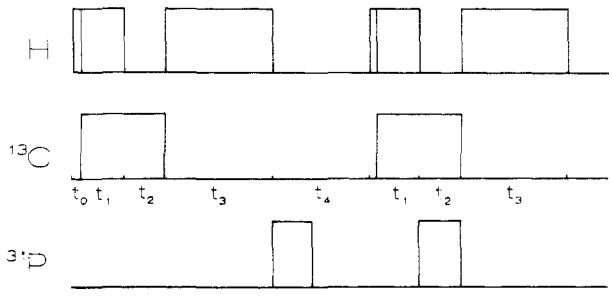

Figure 1. Pulse sequence for direct difference ^1H–^{13}C–^{31}P DCP/MAS ^{13}C NMR: t_0, $\pi/2$ ^1H pulse; t_1, spin lock ^1H–^{13}C cross-polarization contact time; t_2, ^{13}C spin lock hold time in the first half of the sequence and ^{13}C–^{31}P cross-polarization contact time in the second half; t_3, ^{13}C FID acquisition time; t_4, recycle delay. Typical ^1H–^{13}C and ^{13}C–^{31}P cross-polarization contact times are 1–3 and 10–30 ms, respectively. Typical H_1 amplitudes are 40–60 kHz. All pulses have constant amplitudes that satisfy eq 1. The ^{31}P radio frequency pulses may be phase modulated by coherent $0_r/180_r°$ phase alternation at rates $(2t)^{-1}$ = 1–20 kHz.

pulser. The probe (Doty Scientific, Inc.) was a triple-tuned (200, 81, 50 MHz) single-coil design with an H_1 amplitude limit of ca. 80 kHz for ^{13}C–^{31}P cross polarization. The sample was contained in a cylindrical, sapphire, double-bearing rotor with an internal volume of 130 μL.

^1H–^{13}C–^{31}P DCP/MAS ^{13}C NMR experiments were performed with use of the direct difference DCP pulse sequence in Figure 1, based on that given by Schaefer et al.[5] The sequence cycle contains two acquisition periods, t_3. The first part of the sequence is a conventional ^1H–^{13}C cross-polarization experiment with the carbon magnetization held in a spin-locked state for t_2 prior to acquisition. The second part, identical with the first on the ^1H and ^{13}C channels, incorporates a ^{13}C–^{31}P cross-polarization contact during t_2 which depletes carbon magnetization from the ^{13}C spin lock field. Subtraction of the second FID from the first yields the ^{13}C–^{31}P cross-polarization signal. A ^{31}P radio frequency pulse is applied in the first half of the sequence, following acquisition, to balance radio frequency heating.

Two direct difference DCP experiments were used which differ with respect to the implementation of phase modulation of the ^{31}P H_1 field during the ^{13}C–^{31}P cross-polarization interval. The distinction between these experiments is indicated by specifying the phase modulation rate, X kHz, in the shorthand notation DCP(X). A coherent phase modulation scheme was used consisting of a continuous train of radio frequency pulses of duration t with alternating 0/180° phase. Modulation rates $(2t)^{-1}$ = 1–20 kHz span the region of interest.

Phosphorus and carbon H_1 amplitudes were determined relative to the proton H_1 amplitude, derived from the 90° ^1H pulse length measurement. The ^1H–^{13}C cross-polarization match condition[4] (eq 1, i = H) was set by

$$\nu_{1C} = (\gamma_C/2\pi)H_{1C} = (\gamma_i/2\pi)H_{1i} = \nu_{1i} \qquad (1)$$

mapping the ^{13}C CP intensity of hexamethylbenzene as a function of ^{13}C H_1 amplitude (0.1-dB increments) and choosing the match at the first higher H_1 MAS side band. The ^{13}C–^{31}P match condition (eq 1, i = P) was set by mapping $^{13}C(9)$ DCP(0) signal intensity in dimethyl ([9-^{13}C]-9-methylfluoren-9-yl)phosphine oxide (**1**) as a function of ^{31}P H_1 amplitude, ^1H and ^{13}C H_1's being held constant, and selecting the first higher H_1 MAS sideband. MAS speed for related experiments was maintained at the same value ±20 Hz. All proton pulses use the same level H_1 field.

The dipolar coupling between a ^{13}C–^{31}P pair with internuclear distance typical for two- and three-bond separations is several hundred hertz. For cross polarization between these nuclei eq 1 nominally must be satisfied to within the magnitude of the ^{13}C–^{31}P dipolar coupling. Stability of the ratio H_{1C}/H_{1P} on the order of 250 Hz/ 50 kHz, i.e., ca. 0.5%, can be difficult to maintain for extended times. In DCP(0) experiments the amplitudes of the ^{13}C and ^{31}P H_1 fields were monitored continuously and adjusted to maintain a constant ratio.

Synthesis. Melting points were determined on a Thomas Hoover capillary apparatus and are corrected. Literature melting points are for substances with ^{13}C at natural abundance. Solution NMR spectra were determined on a Varian FT-80 NMR spectrometer. ^1H and ^{13}C NMR chemical shifts are on the TMS scale (secondary ^{13}C chemical shift references: $CDCl_3$, δ 76.9 ppm; DMSO-d_6, δ 39.5 ppm). ^{31}P NMR chemical shifts are relative to external H_3PO_4. Digital resolution in the ^{13}C and ^{31}P spectra equals 2 Hz/point, giving J ±2 Hz. Elemental analyses were performed by Galbraith Laboratories, Inc., Knoxville, TN.

Chart I

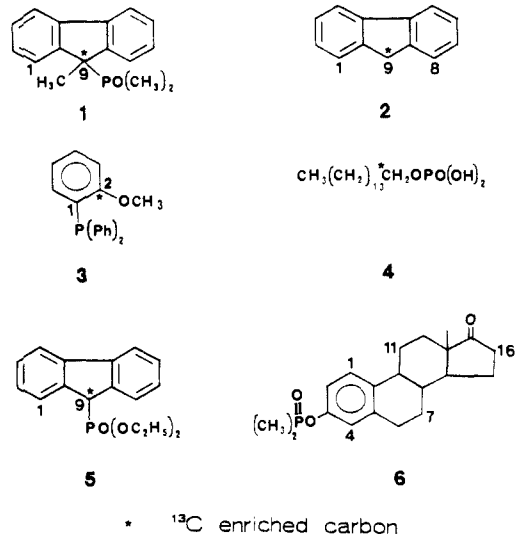

Dimethyl([9-^{13}C]-9-methylfluoren-9-yl)phosphine Oxide (1). [9-^{13}C]-9-Methylfluorene (5.2 mmol), prepared by inverse quench of the lithio anion of [9-^{13}C]-fluorene[6] (90.2 atom % ^{13}C) in an excess of methyl iodide, was dissolved in dry THF at 0 °C. A solution of *n*-BuLi (1.6 M in hexane, 5.7 mmol) was added and the mixture was stirred 1 h, under argon. Dimethylphosphinic chloride (1.45 M in THF, 5.7 mmol) was added and the mixture was stirred for an additional 2 h. Water (25 mL) was added and the pH was adjusted to 7. The solution was evaporated under reduced pressure to remove most of the THF, and the remaining solution was extracted with benzene, dried (Na_2SO_4), and evaporated. Crystallization from ethyl acetate yielded **1**: mp 173.5–175 °C; ^{13}C NMR ($CDCl_3$) 144.7 (C, $^1J_{CC}$ = 40 Hz, C8a, C9a), 139.8 (C, C4a, C4b), 127.3 (CH), 126.8 (CH), 124.4 (CH), 119.5 (CH), 52.2 (C, $^1J_{CP}$ = 59 Hz, C9), 17.0 (CH_3, $^1J_{CC}$ = 33 Hz, 9 CH_3), 11.8 (CH_3, $^1J_{CP}$ = 68 Hz). Anal. ($C_{16}H_{17}OP$) C, H, P.

([2-^{13}C]-2-Methoxyphenyl)diphenylphosphine (3). The Grignard reagent prepared from [1-^{13}C]-2-bromoanisole was treated with chlorodiphenylphosphine according to a literature procedure[7] to provide **3**. The labeled anisole was derived from [1-^{13}C]-4-nitrophenol by O-methylation (CH_2N_2), monobromination (neat Br_2),[8] reduction of the nitro group ($SnCl_2$/HCl),[8] and finally diazotization and reduction (H_3PO_2).[9] The [1-^{13}C]-4-nitroanisole was prepared from the condensation of sodium nitromalonaldehyde[10] and [2-^{13}C]-acetone (99% ^{13}C).[11] **3**: mp 122.0–122.5 °C (lit.[7] mp 122.5–123.5 °C); ^{13}C NMR ($CDCl_3$) 160.8 (C, $^2J_{CP}$ = 15 Hz, C2), 136.6 (C, J_{CP} = 10 Hz, C1′, C1″), 133.9 (CH, $^2J_{CP}$ = 10 Hz, C6), 133.8 (CH, $^2J_{CP}$ = 20 Hz, C2′, C2″), 130.2 (CH, C4), 128.4 (CH, C4′, C4″), 128.2 (CH, $^3J_{CP}$ = 7 Hz, C3′, C3″), 125.5 (C, J_{CP} = 16 ± 4 Hz, J_{CC} = 72 ± 4 Hz, C1), 120.9 (CH, C5), 110.1 (CH, J_{CC} = 67 Hz, C3), 55.5 (CH_3). Anal. ($C_{19}H_{17}OP$) C, H, P.

[1-^{13}C]-1-Pentadecyl Dihydrogen Phosphate (4). Catalytic hydrogenolysis of the [1-^{13}C]-1-pentadecyl diphenyl phosphate (PtO/HOAc), obtained from diphenyl phosphorochloridate and [1-^{13}C]-1-pentadecanol,[12] gave **4**. The labeled alcohol was made by carbonation (98.3% $^{13}CO_2$) of the Grignard reagent prepared from tetradecyl bromide, followed by $LiAlH_4$ reduction of the [1-^{13}C]-pentadecanoic acid. **4**: mp 76–77 °C; ^{13}C NMR (DMSO-d_6) 65.5 (C1), 31.6 (C13), 30.4 (J_{CC} = 36 ± 4 Hz, one half of doublet hidden under the 29.4-ppm peak, C2), 29.4 (C4–C12), 25.3 (C3), 22.4 (C14), 13.9 (C15). Anal. ($C_{15}H_{33}O_4P$) C, H, P.

Diethyl ([9-^{13}C]-fluoren-9-yl)phosphinate (5). 9-Bromo-[9-^{13}C]-fluorene (0.80 g, 3.26 mmol), prepared by bromination (NBS)[13] of [9-

(5) Schaefer, J.; McKay, R. A.; Stejskal, E. O. *J. Magn. Reson.* **1979**, *34*, 443–447.

(6) Chambers, R. R., Jr.; Hagaman, E. W.; Woody, M. C.; Smith, K. E.; McKamey, D. R. *Fuel* **1985**, *64*, 1349–1354.

(7) McEwen, W. E.; Shiau, W.-I.; Yeh, Y.-I.; Schulz, D. N.; Pagilagan, R. U.; Levy, J. B.; Symmes, C., Jr.; Nelson, G. O.; Granoth, I. *J. Am. Chem. Soc.* **1975**, *97*, 1787–1794.

(8) Piutti, A. *Chem. Ber.* **1897**, *30*, 1170–1174.

(9) Adams, R.; Kornblum, N. *J. Am. Chem. Soc.* **1941**, *63*, 188–200.

(10) Fanta, P. E. In *Organic Syntheses*; Rabjohn, N., Ed.; John Wiley & Sons, Inc.: New York, 1963; Collect. Vol. IV, pp 844–845.

(11) Kratzl, K.; Vierhapper, F. W. *Monatsh. Chem.* **1971**, *102*, 224–232.

(12) Brown, D. A.; Malkin, T.; Maliphant, G. K. *J. Chem. Soc.* **1955**, 1584–1588.

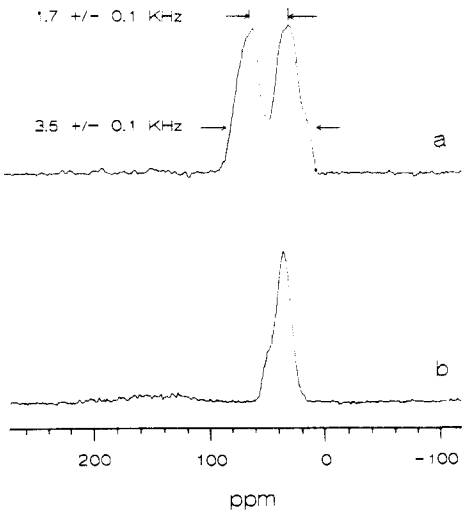

Figure 2. ^{1}H–^{13}C CP ^{13}C NMR spectra of nonspinning microcrystalline samples of **1** (a) and **2** (b). The latter spectrum depicts the nearly axially symmetric CSA powder pattern of the $^{13}C(9)$ resonance of fluorene. The ^{31}P–^{13}C dipolar coupling, D_{CP}, evaluated at the cusps of the dipolar powder doublet (θ = 90°, eq 2) of spectrum a is 1.7 ± 0.1 kHz.

^{13}C]-fluorene (90.2 atom % ^{13}C) and triethyl phosphite (0.6 mL, 3.5 mmol) were refluxed overnight with use of an air-cooled Vigreaux column and slow argon sweep to allow ethyl bromide to escape. The red oil obtained on cooling was chromatographed on silica gel (60–200 mesh) with 30% CH_2Cl_2/hexane, which elutes fluorene and bromofluorene. The column was then eluted with ethyl acetate, which yielded **5** as a clear oil that crystallized after all solvent was removed under vacuum. Recrystallization from hexane/cyclohexane or sublimation gave pure **5**: mp 41.0–42.5 °C. ^{1}H NMR 7.1–7.8 (m, 8 H), 4.45 (d, $^{2}J_{HP}$ = 30 Hz), 3.63–4.00 (m, 4 H), 1.01 (t, J = 7 Hz); ^{13}C NMR ($CDCl_3$) 141.3 (C, C4a, C4b), 138.4 (C, J_{CC} = 38 Hz, C1a, C8a), 127.5 (CH), 126.8 (CH), 126.0 (CH), 46.8 (CH, $^{1}J_{CP}$ = 136 Hz, C9), 62.4 (CH_2), 15.9 (CH_3); ^{31}P NMR 38.8 ($^{2}J_{PH}$ = 30 Hz). Anal. ($C_{17}H_{19}O_3P$) C, H, P.

Results and Discussion

The heteronuclear dipole–dipole interaction between a ^{13}C and ^{31}P nuclear pair, D_{CP}, is

$$D_{CP} = (\gamma_C\gamma_P\hbar/2\pi r_{CP}^3)(1 - 3\cos^2\theta) \qquad (2)$$

where γ_C and γ_P are the ^{13}C and ^{31}P gyromagnetic ratios, respectively, r_{CP} is the ^{13}C–^{31}P internuclear distance, and θ is the angle between the internuclear axis and the external magnetic field axis. This fundamental relationship between dipolar coupling and internuclear distance is not used routinely in ^{13}C NMR molecular structure analysis as the experimental measurement of D is complicated by multiple line width contributions and the overlap of line shapes from chemically shifted carbon centers.

Dipolar coupling is apparent in static spectra when this interaction is the dominant line-broadening mechanism and a single dipolar interaction is selected by specific enrichment. Figure 2a shows the spectrum of dimethyl([9-^{13}C]-9-methylfluoren-9-yl)-phosphine oxide (**1**) and Figure 2b shows the spectrum of [9-^{13}C]-fluorene (**2**), recorded on static, microcrystalline powder samples. Resonances from the natural abundance aromatic carbons are discernable in both spectra as a broad ca. 200-ppm low-intensity signal on the baseline. The resonance at 40 ppm in the spectrum of **2** is from $^{13}C(9)$. The narrow chemical shift anisotropy (CSA) powder line shape of this sp^3-hybidized carbon resonance is nearly axially symmetric: $\sigma_\parallel - \sigma_\perp \approx 14$ ppm. The static spectrum of C(9) of **1** will have a CSA powder line shape comparable to **2** and dipolar coupling with the phosphorus. The superimposed axially symmetric ^{31}P–^{13}C dipolar powder patterns for the $+^1/_2$ and $-^1/_2$ ^{31}P spin states generate a broad doublet, with peak separation of 1.7 ± 0.1 kHz and maximum width of 3.5 ± 0.1 kHz. These values correspond to D_{CP} (1.8 kHz) and $2D_{CP}$ (3.6 kHz) evaluated from eq 2 with r_{CP} = 0.19 nm (estimate)

(13) Wittig, G.; Felletschin, G. *Liebigs Ann. Chem.* **1944**, *555*, 133–145.

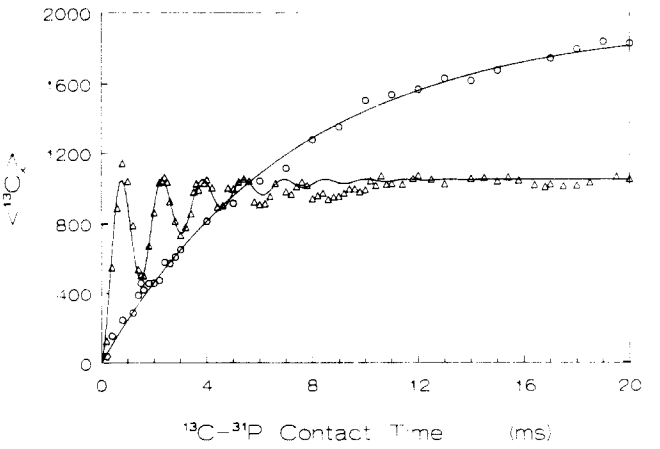

Figure 3. DCP carbon signal intensity, $\langle^{13}C_x\rangle$, for $^{13}C(9)$ of **1** as a function of ^{13}C–^{31}P cross-polarization contact time, t_2. The data are from experiments employing 61 kHz H_1 fields and MAS = 2.9 kHz. Triangles are data points from DCP(0); the function drawn through these points is $\langle^{13}C_x\rangle = 1050(1 - 0.5e^{-t/0.0025} - 0.5e^{-t/0.0025}\cos(4080t))$. Circles are data points from DCP(20); the function through these points is $\langle^{13}C_x\rangle = 1940(1 - e^{-t/0.0074})$.

and θ = 90 and 0°, respectively.[14]

The maximum width of the dipolar powder pattern for coupled ^{13}C–^{31}P spins separated by two bonds (r_{CP} = 0.31–0.39 nm) = 400–800 Hz. In the presence of large CSA, typically 160–200 ppm (8–10 kHz at 4.7 T) for aromatic carbons,[15] weak dipolar interactions will not be apparent by inspection of the static spectrum and a moment analysis is the most direct way to determine the heteronuclear dipolar coupling.[3a]

T_{CP} Measurements. DCP uses two sequential cross-polarization steps. The first is between the protons in the system and one of the dilute nuclei (^{13}C, ^{31}P) and is accomplished with conventional, matched Hartmann–Hahn spin-lock cross-polarization methods.[16] Its function is to generate efficiently a dilute nucleus magnetization similar to that observed in a long recycle Bloch decay experiment.[17] The cross-polarization process from protons, dipolar coupled among themselves and hence characterized by a common spin temperature and large heat capacity, to a dilute nucleus, e.g., ^{13}C, is commonly found to exhibit theoretically expected exponential dynamics.[18] In the present work the second cross-polarization step is between the two rare nuclei, by virtue of low natural abundance (^{13}C) and chemical dilution (^{31}P). As proximate ^{13}C and ^{31}P pairs are spatially isolated from homonuclear spins and simultaneously decoupled from heteronuclear interactions with the lattice protons by the spin-locking fields, they approximate isolated spin pairs. In this two-spin system, the magnetization transfer process via matched Hartmann–Hahn spin-lock cross polarization may exhibit an oscillatory behavior as the polarization shuttles between the connected spin pair. Strong oscillations in $\langle^{13}C_x\rangle$ which occur during cross polarization between isolated spin $^1/_2$ pairs (^{13}C, ^{1}H) were observed in *nonspinning* experiments performed on *single crystals* and were shown to arise from heteronuclear dipolar coupling.[19–21] A theoretical treatment of the

(14) Maciel, G. E. In *Magnetic Resonance: Introduction, Advanced Topics and Applications to Fossil Energy*; Petrakis, L., Fraissard, J. P., Ed.; D. Reidel Publishing Company: Dordrecht, Holland, 1984; NATO ASI Series C, Vol. 124, pp 71–110.

(15) Pausak, S.; Tegenfeldt, J.; Waugh, J. S. *J. Chem. Phys.* **1974**, *61*, 1338–1344.

(16) Mehring, M. *High Resolution NMR Spectroscopy in Solids*; Diehl, P., Fluck, E., Kosfeld, R., Eds.; Springer-Verlag: Berlin, 1976; NMR-Basic Principles and Progress, Vol. 11, Chapter 4.

(17) Alemany, L. B.; Grant, D. M.; Pugmire, R. J.; Alger, T. D.; Zilm, K. W. *J. Am. Chem. Soc.* **1983**, *105*, 2133–2141.

(18) Pines, A.; Gibby, M. G.; Waugh, J. S. *J. Chem. Phys.* **1973**, *59*, 569–590.

(19) Muller, L.; Kumar, A.; Baumann, T.; Ernst, R. *Phys. Rev. Lett.* **1974**, *32*, 1402–1406.

(20) Hester, R. K.; Ackerman, J. L.; Cross, V. R.; Waugh, J. S. *Phys. Rev. Lett.* **1975**, *34*, 993–995.

time evolution of $\langle^{13}C_x\rangle$ in these experiments predicted that the oscillation frequency of the magnetization in these experiments was proportional to D_{CH}, specifically, $\nu = D_{CH}/2$.[19]

Similar oscillations are observed during cross polarization between isolated ^{13}C–^{31}P spin pairs in *spinning* experiments on *microcrystalline powder samples*. A plot of carbon signal intensity, $\langle^{13}C_x\rangle$, for C(9) of **1** vs ^{13}C–^{31}P contact time, acquired with use of DCP(0) (Figure 3, Δ's), illustrates this response. The oscillation period is 1.54 ms and is independent (±0.1 ms) of resonance offsets <2.5 kHz for the ^{13}C and/or ^{31}P radio frequency fields with typical H_1's of 50–60 kHz. For MAS speeds in the range 3–6 kHz, i.e., MAS > D_{CP}, the oscillation frequency is independent of the spinning speed. Similarly, it is not a function of the amplitude of the H_1's in the range 40–65 kHz. Hence, the oscillations do not appear related to experimental variables. In analogy with static experiments on isolated spin pairs in single crystals, the oscillations are attributed to the dipolar interaction between the nuclei. While the dipolar coupling per se is not apparent in the high-resolution (D)CP/MAS ^{13}C NMR spectrum, the interaction does not vanish under MAS, as evidenced by efficient cross polarization between these nuclei. The DCP(0) data in this figure are fit by

$$\langle^{13}C_x\rangle = A(1 - 0.5e^{-t/T} - 0.5e^{-t/T}\cos\omega t) \qquad (3)$$

with the constants $A = 1050$, $T = T_{CP} = 2.5$ ms, and $\omega = 4080$ rad s^{-1}, respectively. Within the precision of the data, the ^{13}C–^{31}P cross-polarization rate and the oscillation decay rate are the same. The ratio of the oscillation frequency $\nu = \omega/2\pi = 650 \pm 40$ Hz and the independently measured value of $D_{CP} = 1.7 \pm 0.1$ kHz yields the proportionality constant between these quantities; $\nu/D_{CP} = 0.38 \pm 0.02$.

The $^{13}C(2)$–^{31}P cross-polarization oscillation frequency observed in **3** is 240 ± 40 Hz. The larger error associated with this measurement, relative to that in **1**, results from fewer $\langle^{13}C_x\rangle$ data points (0.5-ms increments in t_2) in the definition of ν. This value and the above proportionality constant yield $D_{CP} = 632 \pm 105$ Hz, and, by eq 2, $r_{CP} = 0.270 \pm 0.015$ nm. This measurement compares favorably with the $^{13}C(2)$–^{31}P internuclear distance of 0.275 ± 0.001 nm determined from the X-ray crystal structure.

Stejskal et al. have shown that transient oscillations in DCP signal intensity can be suppressed by phase modulation of the H_1 field of the unobserved, high-spin-temperature nucleus.[3] The technique experimentally impresses a short $T_{1\rho}$ on the phase-modulated spin system. With $T_{1\rho} \ll T_{CP}$ the magnetization dephases more rapidly than it accrues and the reverse transfer is quenched. With this modification the cross-polarization process exhibits exponential kinetics. This is shown by the data in Figure 3 collected with DCP(20). Relative to DCP(0), DCP(X) produces a larger ^{13}C magnetization since the transfer is driven unidirectionally.

The ^{13}C–^{31}P cross-polarization time, T_{CP}, evaluated from the DCP(0) data on **1** (Figure 3) is 2.5 ms. The apparent T_{CP} measured in DCP(X) experiments is longer than this value and dependent on the ^{31}P radio frequency phase modulation rate. T_{CP} increases from 3 ± 1 to 5 ± 1 to 8 ± 1 ms for modulation rates of 5, 10, and 20 kHz, respectively. Cross-polarization rates are proportional to the strength of the dipolar coupling times the spectral density overlap of the ^{13}C and ^{31}P rotating frame Larmor frequencies.[3a] The modulation imposes an uncertainty broadening on ν_{1P} that decreases the overlap term (at the optimum match frequency measured in the absence of phase modulation) and produces the slowed $(T_{CP})^{-1}$'s.

The Hartmann–Hahn Match Condition in DCP(X) Experiments. Magic angle spinning modulates the heteronuclear dipolar interaction so that cross polarization occurs at $\Delta = \pm\nu_s, \pm 2\nu_s$, where ν_s is the spinning frequency and Δ is the deviation from the static Hartmann–Hahn matching condition.[22] Heteronuclear dipolar interactions are fully amplitude modulated with suppressed

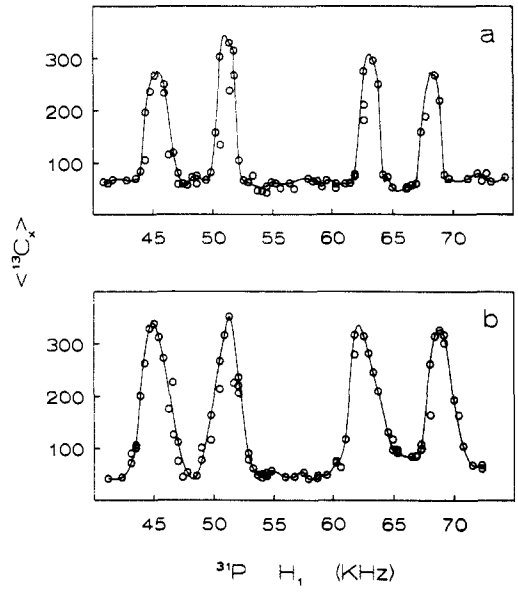

Figure 4. DCP(0) carbon signal intensity, $\langle^{13}C_x\rangle$, vs ^{31}P H_1 amplitude for the ^{13}C-enriched site of (a) **3** and (b) **4** with the following parameters: ^1H–^{13}C and ^{13}C–^{31}P cross-polarization contact times of 1 and 15 ms, respectively. Hartmann–Hahn match: 63 kHz at $\Delta = \nu_s = 6050 \pm 20$ Hz.

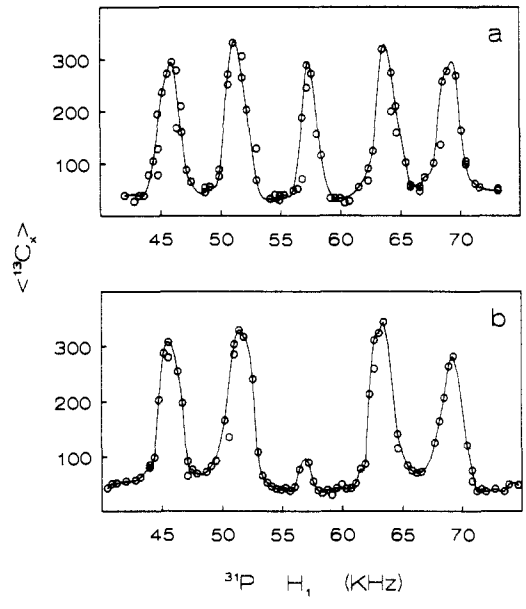

Figure 5. DCP(0) carbon signal intensity, $\langle^{13}C_x\rangle$, vs ^{31}P H_1 amplitude for the ^{13}C-enriched site of (a) **5** and (b) **1**. Experimental parameters as listed in Figure 4.

polarization transfer at Δ = 0. This is illustrated in Figure 4, which shows plots of carbon signal intensity vs ^{31}P H_1 amplitude for ([2-^{13}C]-2-methoxyphenyl)diphenylphosphine (**3**) and [1-^{13}C]-1-pentadecyl dihydrogen phosphate (**4**) measured with DCP(0). In each substance the carbon magnetization plotted is that of the ^{13}C enriched site; maximum signal intensity for each substance has been scaled to comparable height. The cross-polarization peaks shown in this plot were obtained with a 15-ms ^{31}P–^{13}C cross-polarization contact time, ca. one cross polarization time constant for the weakly coupled dipole pair in **3** and **4**. In this time regime signal intensities (the ordinate in Figures 4 and 5) are an approximate reflection of rate. The cross-polarization rate for the amplitude-modulated ν_s:$2\nu_s$ MAS side bands has a theoretical ratio of 1:0.7.[22] Data points were determined in an interleaved order, holding the ^1H and ^{13}C H_1 amplitudes constant at 63 kHz (the preset ^1H–^{13}C cross-polarization match condition for the high-field ν_s side band; MAS = 6050 Hz) and varying the ^{31}P H_1 amplitude. The plots appear symmetrical about the static

(21) Takegoshi, K.; McDowell, C. A. *J. Chem. Phys.* **1987**, *86*, 6077–6084.
(22) Stejskal, E. O.; Schaefer, J.; Waugh, J. S. *J. Magn. Reson.* **1977**, *28*, 105–112.

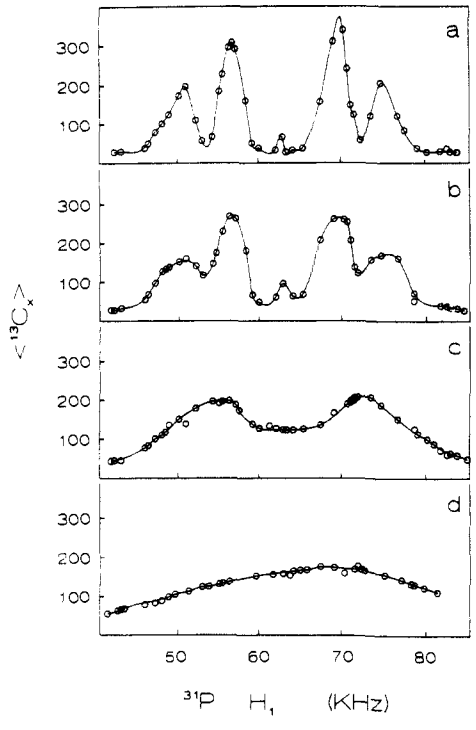

Figure 6. DCP(X) carbon signal intensity, $\langle^{13}C_x\rangle$, vs ^{31}P H_1 amplitude for C(2) of **3** for four ^{31}P H_1 phase modulation rates (kHz): X = 1 (a), 2 (b), 5 (c), 10 (d). Experimental parameters: ^1H–^{13}C and ^{13}C–^{31}P cross-polarization contact times = 1 and 15 ms, respectively; Hartmann–Hahn match: 69 kHz at $\Delta = \nu_s$ = 6090 ± 20 Hz.

Hartmann–Hahn match condition of 57 kHz.

Figure 5 presents $\langle^{13}C_x\rangle$ vs ^{31}P H_1 plots for the ^{13}C-enriched carbon of diethyl ([9-^{13}C]-fluoren-9-yl)phosphinate (**5**) (a) and (**1**) (b), determined under the same conditions described in Figure 4. Both substances contain a directly bonded ^{13}C–^{31}P pair with similar and near-maximum dipolar coupling. In addition to the peaks at ν_s and $2\nu_s$, both of these substances show ^{13}C cross-polarization signal intensity at Δ = 0. This peak has its origin in the frequency modulation of the ^{13}C–^{31}P dipolar coupling by the homonuclear ^1H dipolar interaction.[22] In **5**, the ^{31}P–$^{13}C(9)$ dipole pair is tightly coupled to the proton spin system through H(9) and the resulting modulation results in cross-polarization efficiency at the static match condition comparable to that observed at the $2\nu_s$ side band maxima. Both ^{31}P and $^{13}C(9)$ in **1** are nonprotonated and therefore coupled weakly to the proton spin system, relative to **5**. This compound shows intermediate behavior with weak cross polarization at Δ = 0.

The width of the peaks in Figures 4 and 5 reflects the fact that ν_1 in eq 1 is not a unique frequency but rather a spectral density function centered on ν_1. Residual dipolar coupling to protons arising from incomplete decoupling of the proton spin system from the ^{13}C and ^{31}P nuclei is an important contributor to the width of the spectral density function. The half-height peak widths of **1**, **4**, and **5** are comparable, about 2 kHz. The peak widths for **5** and **1** are similar despite the fact that ^{13}C in **5** is protonated while ^{13}C in **1** is not. The contribution to the widths from residual coupling to protons may be masked by an experimental broadening effect. It is difficult to maintain precise control of the H_1 amplitudes over the several hours required for data collection in these experiments. The significant scatter in the data in Figures 4 and 5 results from this instability. Rapid simultaneous mapping of $\langle^{13}C_x\rangle$ vs ^{31}P H_1 for **3** and **5** from a rotor packed with a mixture of both substances shows that the half-height peak width for **3** is ca. 25% less than that for **5**. In this comparison residual coupling to protons and ^{13}C–^{31}P dipolar coupling are strong in **5** and weak in **3**.

As indicated above, introduction of ^{31}P H_1 phase modulation to achieve exponential cross-polarization dynamics lengthens the apparent cross-polarization rate. This is shown graphically in Figure 6, a plot of DCP(X) carbon signal intensity vs ^{31}P H_1 amplitude for X = 1, 2, 5, and 10 kHz for the ^{13}C-enriched resonance of **3**. In this figure the ordinate is intensity. The general correspondence of intensity and rate profiles for **3** has been verified separately by $(T_{CP})^{-1}$ measurements for the DCP(2) experiment of Figure 6. As the modulation rate is increased from 1 to 10 kHz, the $(T_{CP})^{-1}$ maxima decrease as the peak widths increase (by approximately the modulation rate). The sharp peaks at $\Delta = \nu_s, 2\nu_s$ observed without the ^{31}P H_1 modulation, Figure 4a, coalesce with 5-kHz modulation, Figure 6c, so that $(T_{CP})^{-1}$ becomes much less sensitive to small variations in the ^{31}P H_1 amplitude. For DCP(10) the rate becomes virtually insensitive to the match condition (±1 kHz), an independence gained at the further expense of decreased cross-polarization rate.

Long ^{13}C $T_{1\rho}$'s are required for optimum sensitivity in DCP experiments and are under experimental control through their dependence on H_1 amplitude. This is not a limiting parameter for most organic substances that typically have ^{13}C $T_{1\rho}$ values tens to hundreds of milliseconds long in 40–50-kHz spin-lock fields. Materials that have inherently short $T_{1\rho}$, e.g., by virtue of motion or high free electron spin density, require the highest achievable H_1's to maximize the DCP volume element. Design constraints of the triple tuned probe can limit the high H_1 amplitude and/or the cross-polarization contact interval. This can compromise the accurate determination of $(T_{CP})^{-1}$'s for interactions separated by two or more bonds by preventing signal intensity measurements over several time constants. This situation is made worse by the experimentally imposed rate decrease that accompanies ^{31}P H_1 phase modulation. In general, the apparent $(T_{CP})^{-1}$ should be as fast as possible consistent with maintaining the ratio of H_1 amplitudes dictated by eq 1. Phase modulation of 5 kHz is sufficient to broaden the ^{31}P–^{13}C match condition so that the rare spin nuclei H_1's can be held within acceptable tolerances (±0.3 dB) for long-term measurements with use of commercial equipment, i.e., without active monitoring and control of H_1 amplitudes. The modulation simulatneously relaxes precise MAS speed constraints implicit in DCP(0) experiments (Figures 4 and 5) required for optimum signal detection. MAS speed regulation to ±20 Hz results in a shift of ≤±0.1 dB in the optimum match condition, an acceptable variation in DCP(5) experiments.

The ^{31}P–^{13}C cross-polarization rate is proportional to the square of the dipolar coupling,[18] eq 2, and therefore exhibits and r_{CP}^{-6} dependence. Typical internuclear distances (nm) for pairs separated by one (0.19), two (0.28), three (0.31-short, 0.39-long), and four (0.45-short) bonds predict nominal rate ratios, relative to the rate for a directly bonded pair, of 1.0:0.1:0.05, 0.01:0.005, respectively. These values are approximate since rates are also proportional to the spectral density overlap term which need not be constant for all carbon centers in the cross-polarization sphere. A comparison of the conventional CP/MAS and DCP/MAS ^{13}C NMR spectra of estrone dimethylphosphinate (**6**) is presented in Figure 7. The DCP spectrum (Figure 7a) reveals the methyls attached to phosphorus, the oxygenated aromatic carbon, and its ortho neighbors and shows excellent discrimination against resonances beyond the third bonding sphere. Intensity ratios of these DCP signals are in qualitative agreement with the predictions based on T_{CP}^{-1}. Chemical shift data and protonation state of the carbons of the DCP resonances,[2] here elicited from **6**, but potentially arising from a component of a complex mixture, identify a phenolic site with unsubstituted ortho positions and without oxygen or nitrogen heteroatoms in the meta or para positions.

Conclusions

The DCP NMR technique in general and the specific version presented in this report are examples of a powerful set of solid-state NMR experiments that utilize the heteronuclear dipolar interaction to elicit an NMR response from local sites within a solid organic matrix. The selection criteria, cross polarization via dipolar coupled pairs, reveal the local bonding arrangement around select heteroatoms in the system. With cross-polarization rates governed by an inverse sixth-power dependence on internuclear distance, DCP siganls in the ^1H–^{13}C–^{31}P DCP/MAS ^{13}C NMR experiment are constrained to a spherical volume element of 0.4-nm radius

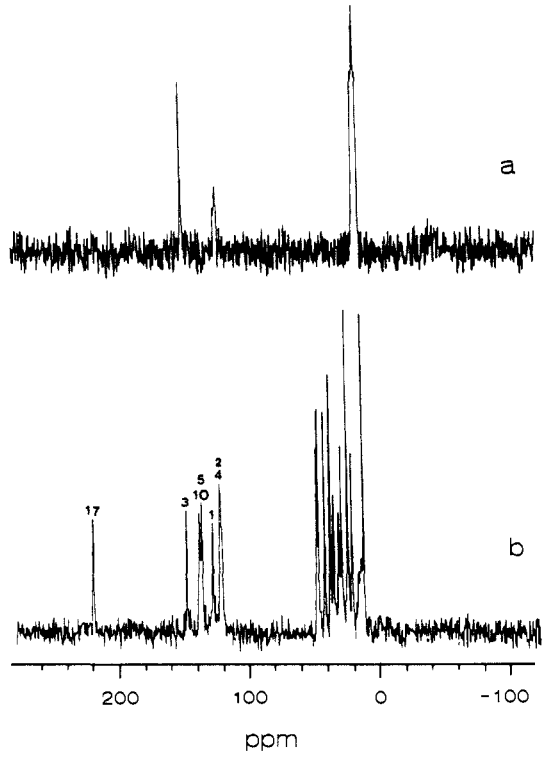

Figure 7. (a) $^{1}H-^{13}C-^{31}P$ DCP/MAS ^{13}C NMR spectrum of **6** recorded with DCP(5) and a 15-ms $^{13}C-^{31}P$ contact time; (b) $^{1}H-^{13}C$ CP/MAS ^{13}C NMR spectrum of **6**. Chemical shift assignments from low to high field are as follows: 219.4 (C17), 148.2 (C3), 138.6 (C5)[a], 136.8 (C10)[a], 128.4 (C1), 122.0 (C4), 122.0 (C2), 48.5 (C14)[b], 48.0 (C13)[b], 43.1 (C9), 39.0 (C8), 36.6 (C16), 32.1 (C12), 30.3 (C6), 25.6 (C7), 25.6 (C11), 22.4 (C15), 16.8 ($-PCH_3$), 15.7 ($-PCH_3$), 13.5 (C18). Carbons indicated with common superscripts may have assignments interchanged.

around the phosphorus atom. This allows observation of resonances in the first, second, and third bonding sphere from the phosphorus; assignment to these spheres is possible on the basis of relative cross-polarization rates. While the 0.4-nm distance is a soft boundary condition, *inter*molecular contacts between the phosphorus and carbon generally exceed this limit. The low T_{CP}^{-1} for carbons >0.4 nm from the phosphorus atom is the practical basis for the assertion that this experiment is an *intra*molecular structure probe. This underlies the interpretation of DCP spectra of unknowns and/or mixtures for which the goal is the definition of statistical, primary structure within the $^{13}C-^{31}P$ cross-polarization sphere.[23]

The version of the DCP experiment with ^{31}P radio frequency phase modulation, DCP(X), is easily executed without special control of the H_1 amplitude and MAS speed. It is the experiment of choice for survey spectra that define the carbon bonding configuration around the heteroatom. The DCP(5) experiment embodies an acceptable compromise between experimental ease and efficiency, with T_{CP}^{-1}'s lengthened less than 2-fold by the experimentally imposed phase modulation.

The DCP(0) experiment requires careful optimization and control of H_1 amplitude and MAS speed. Its value lies in its ability to provide a measure of the dipolar coupling interaction and, hence, the determination of internuclear distance. The theoretical value of the reduced dipolar interaction observed via oscillatory cross-polarization kinetics between isolated dipole pairs in MAS experiments has not been reported. The DCP(0) results on **1** and the measurement of D_{CP} from the static spectrum yield $\nu/D_{CP} = 0.38 \pm 0.02$, which has been used to determine the $^{13}C(2)-^{31}P$ internuclear distance in **3**.

The utility of the $^{1}H-^{13}C-^{31}P$ DCP/MAS ^{13}C NMR technique lies in its ability to provide structural information at the functional group level in a wide variety of substances that contain phosphorus or that can be chemically labeled with this element. In the latter case the method provides a means to characterize materials based on chemical reactivity and is applicable to homogeneous systems and complex materials (natural and synthetic polymers, blends, fossil fuels). DCP spectra have the nontrivial advantage of being free from solvent and reagent impurities (except those containing phosphorus and carbon) that are often difficult to remove from complex solid mixtures.

Acknowledgment. This work was supported by the Division of Chemical Sciences, Office of Basic Energy Sciences, U.S. Department of Energy, under contract DE-AC05-840R21400 with Martin Marietta Energy Systems, Inc.

(23) Hagaman, E. W. *Energy & Fuels* **1988**, *2*, 861–862.